Cooperative Raman-type transitions in a system of two four-level atoms: Entanglement in the spin subsystem of two spatially separated atomic ensembles

D. V. Kupriyanov, I. M. Sokolov, and A. V. Slavgorodskii
Department of Theoretical Physics, State Technical University, 195251, St. Petersburg, Russia
(Received 6 October 2000; published 14 May 2001)

In this paper we consider the optical coupling of two four-level atoms via cooperative Raman scattering of correlated photons of the nondegenerate spontaneous parametric radiation. The Raman scattering of twin photons incident on the atoms is additionally stimulated by coherent classical radiation in such a way that it is slightly off resonant for each atom considered independently but resonant for the joint system. We discuss the special excitation conditions when the amplitude of the cooperative stimulated Raman scattering from quantum to classical modes becomes greater than the normal transition rates associated with independent Raman scattering. In certain conditions weak entanglement between the Zeeman sublevels in the ground states of these atoms can appear. The small admixture of entanglement in the system of two atoms leads to strong entanglement between transverse macroscopic spin fluctuations of two spatially separated atomic ensembles coupled by such quantum light. The proposed mechanism of entanglement is relevant to the ground state spin subsystem of two distant macroscopic and optically thin atomic ensembles. Such an entangled state can be stored for a long time and used as a basic Einstein-Podolsky-Rosen system in different applications pursuing the goal of spreading quantum information schemes in atomic subsystems.

DOI: 10.1103/PhysRevA.63.063811 PACS number(s): 42.50.Ct, 42.50.Lc, 42.50.Fx

I. INTRODUCTION

Entangled states of elementary subsystems and nonlocal quantum correlations are the most interesting and mysterious features of the general measurement concept of quantum mechanics. The early studies in this fundamental area [1] have led to the emergence of possible practical applications, including quantum cryptography and communication, quantum computation [2–5], and quantum teleportation [6,7]. Up to now the most accessible and controllable sources of the entanglement come from the processes of spontaneous parametric down-conversion in nonlinear optical crystals. Although there are many examples of entanglement in corpuscular matter, such as the electronic shells of atoms or molecules or correlation existing in condensed matter in general, it is hard to extract them and store them for longer times because of dissipation processes. However, if in the experiments it were possible to avoid the dissipation problem then the entanglement in atomic subsystems would definitely find many practically important applications.

An interesting example of entanglement in corpuscular matter, acceptable for experimental realization, can be adopted from the idea of spin squeezing, originally proposed in [8]. Recently it was theoretically predicted and proved by experiment [9] that the atomic ensemble can be squeezed over its macroscopic angular momentum via excitation with squeezed light. The spin squeezing (entanglement) was produced in the upper state and it could not be stored longer than the natural relaxation time. It would be possible to overcome the problem of spontaneous decay if the spin entanglement were realized in the ground state. However, as is well known from many studies of the optical pumping phenomenon [10], the atomic ground state cannot be polarized in one step of optical excitation and spontaneous transitions necessarily contribute to the process of ground state polarization. One possible scheme to create and store macroscopic quantum correlations for an atomic ensemble in the ground state was proposed in Ref. [11]. It was suggested to utilize the Raman-type coupling of Zeeman sublevels in a Λ-type optical configuration. Then, as was shown in Ref. [11], the propagation of both the squeezed and classical light through the optically dense and spin-oriented atomic vapor must lead to squeezing of the transverse spin component. High optical thickness of the atomic vapor was a basic restriction of the idea suggested in Ref. [11].

In the present paper we would like to show that by special optical excitation entanglement can be introduced, in principle, even in a system of two spatially separated atoms. Following Ref. [11] we will consider Raman scattering from the quantum to the classical mode as the basic elementary process. We will show that in certain conditions the amplitude of cooperative scattering by the atoms of the correlated photon pair created in a parametric process can be higher than the corresponding transition probability associated with independent scattering of the photons. It is expected also to be higher than the probability of scattering of photons coming from different pairs or from the noncorrelated part of the radiation spectrum. We will show that such cooperative Raman scattering has a quantum nature and in the example considered in this paper it is based on possible time ordering in the appearance of the photons created in each elementary event of the parametric process.

For a microscopic system consisting of two atoms the admixture of entanglement preserving the purity of the quantum state for the joint system is expected to be weak but not negligible, restricted mainly by the destructive role of the spontaneous processes of Rayleigh and Raman scattering of the classical mode. But this effect can be enhanced many times for spatially separated macroscopic atomic ensembles. In this paper we show that if the ensembles have a strong initial spin orientation then in certain conditions the optical

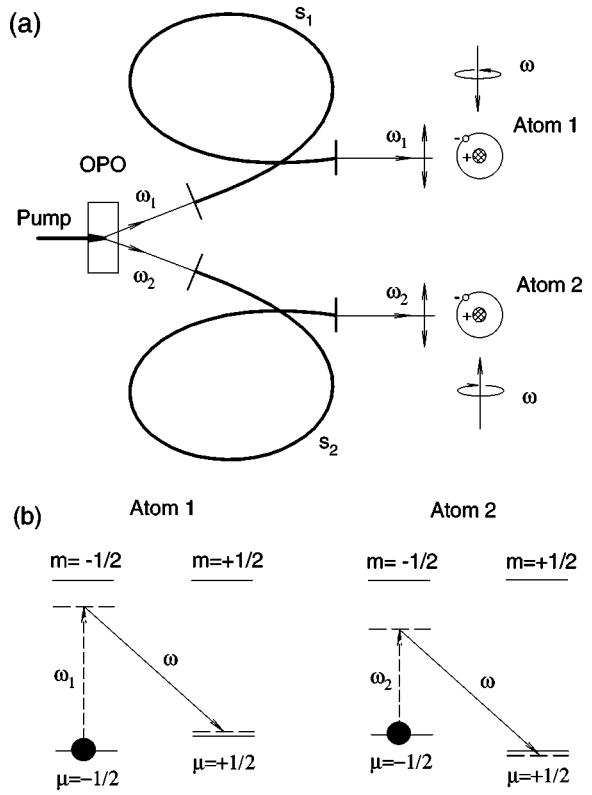

FIG. 1. The proposed scheme of optical coupling between two distant atoms. (a) The linearly polarized OPO modes ω_1 and ω_2, passing the fibers s_1 and s_2, initiate Raman-type transitions in the system of two four-level atoms. The process of Raman scattering is additionally stimulated by the coherent circularly polarized modes ω. (b) The energy level diagram and the participating transitions. The stimulated Raman scattering is slightly off resonant for each atom considered independently but resonant for the joint system.

interaction between them can be described properly by a model of a nondegenerate optical parametric oscillator. In such an interpretation the fluctuations of macroscopic transverse spin components have to be associated with the perturbations of the oscillator's modes. As long as the excitation of the modes has a parametric nature the corresponding quadrature components (i.e., transverse spin fluctuations) become entangled. The proposed mechanism of entanglement is relevant to the spin subsystem of two distant macroscopic but optically thin atomic ensembles. Thus this scheme could be interesting for possible applications dealing with teleportation of quantum systems described by continuum variables (see [7,12–14]). In particular, it should be quite useful in application to the problem of quantum communication between distant atomic ensembles (see [15]).

II. THE PERTURBATION THEORY ANALYSIS

Consider a system of two spatially separated identical atoms located at the points $\mathbf{r}_1$ and $\mathbf{r}_2$ (see Fig. 1). The atoms are modeled as a single electron system with an $s=1/2$ spin ground state and a $j=1/2$ excited state. Such a configuration is typical for D_1 optical transitions in alkali-metal atoms, ignoring their hyperfine structure. Both the atoms initially have strong spin orientation in the ground state and populate only the $\mu=-1/2$ Zeeman state. Then each of the atoms is excited by one mode of a quantum field and by one mode of a coherent classical field. The quantum field is created by the radiation of a nondegenerate optical parametric oscillator (OPO) with two-mode output at frequencies ω_1 and ω_2 [16]. We assume that the first atom is illuminated by the mode ω_1 and the second atom by the mode ω_2 as shown in Fig. 1(a). Both the quantum modes ω_1 and ω_2 have linear polarization and they are applied at the $\mu=-1/2\rightarrow m=-1/2$ optical transition. The coherent mode ω is left-hand circularly polarized and applied at $\mu=+1/2\rightarrow m=-1/2$ [see Fig. 1(b)]. The light beams propagate in orthogonal directions and have different polarizations [see Fig. 1(a)], so there is no overlap in transition matrix elements for the quantum and classical modes.

The key point of our discussion is that we study the Raman scattering shown in Fig. 1(b) when for each of the atoms considered independently there is no resonance for the stimulated process. The Zeeman sublevels of the atoms are split in such a way that the states $\mu=-1/2$ of the first and second atoms are shifted relatively down and up from the states $\mu=+1/2$. However, for the joint system we keep the following four-photon resonance condition:

$$\omega_1+\omega_2=2\omega. \tag{2.1}$$

For clarity we asssume that $\omega_1>\omega_2$ and to simplify our notation we set the following order in the basic states of each atom: $|1\rangle=|s,-1/2\rangle$, $|2\rangle=|s,+1/2\rangle$, $|3\rangle=|j,-1/2\rangle$, $|4\rangle=|j,+1/2\rangle$.

A. Raman scattering by a single atom

Consider first the Raman scattering on each of the atoms independently. In the lowest nonvanishing order of perturbation theory the stimulated scattering of photons from the quantum mode into the coherent mode can be described by the following Keldysh-type diagram:

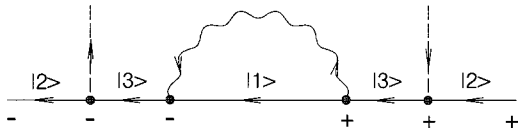

(2.2)

Evaluating this diagram in the off-resonant condition one can estimate the transition rate R (transition probability per unit time) associated with the stimulated Raman process,

$$R\sim\frac{|\Omega'|^2\,\Omega_R^2}{16\,\Delta^2\,\delta^2}\Gamma, \tag{2.3}$$

where Ω_R and Ω' are the Rabi frequencies for classical and quantum modes, $\Delta=\omega-\omega_{32}$ is the optical detuning, $\delta+|\omega_{21}|=\omega_1-\omega=\omega-\omega_2$ is the mode detuning, and Γ is the light induced broadening of the ground state. We assume

that $|\Delta| \gg \delta$ and $\Delta \approx \omega_1 - \omega_{31} \approx \omega_2 - \omega_{31}$. For the circularly polarized classical mode with complex amplitude $\mathcal{E}_0$ the Rabi frequency is given by

$$\frac{\Omega_R}{2} = \frac{1}{\hbar} |d_{23} \mathcal{E}_0|. \tag{2.4}$$

For the linearly polarized quantum mode the Rabi frequency can be expressed in terms of the averaged Heisenberg operators $\epsilon(t)$ as follows:

$$\left(\frac{|\Omega'|}{2} \right)^2 = \frac{1}{\hbar^2} |d_{13}|^2 \langle \epsilon^\dagger(t)\, \epsilon(t) \rangle. \tag{2.5}$$

Here and throughout we denote by d_{ij} (with $i=1,2$ and $j=3,4$) the transition dipole matrix elements. In steady state conditions the right side of Eq. (2.5) should not depend on the time argument t. Also, we omit here the space argument and presume that for close modes $\omega_1 \sim \omega_2$ there is no difference in the Rabi frequencies of quantum fields acting on each atom.

The transition rate (2.3) associated with off-resonant stimulated scattering is expected to be small. Therefore we have to consider also the transitions initiated by spontaneous Raman scattering of the quantum mode into vacuum modes, which have resonance nature. Such a scattering is described by the diagram

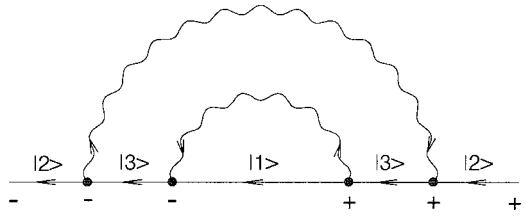

(2.6)

giving the following estimation for the transition rate R'_{sp}:

$$R'_{sp} \sim \frac{|\Omega'|^2\, \gamma_{3\to 2}}{4\, \Delta^2}, \tag{2.7}$$

where $\gamma_{3\to 2}$ is the rate of natural decay in the $|3\rangle \to |2\rangle$ optical transition. In the estimation (2.7) we restricted ourselves to the quasiresonant approximation, assuming $|\Delta| \ll \omega_{31}, \omega_{32}$.

Due to evolution in time after a while atoms will populate sublevel $|2\rangle$ of the ground state. Then the classical mode can be scattered by the atom into the quantum mode because of stimulated scattering as well as into vacuum modes because of spontaneous scattering. Both the processes can be described by one diagram:

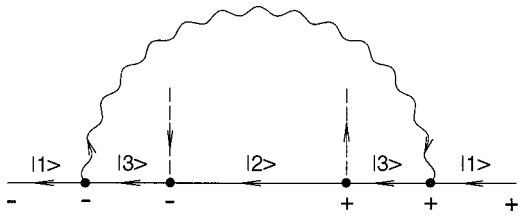

(2.8)

where the stimulated or spontaneous contributions relate to the different domains in the spectrum of the output modes. The rate of stimulated ''back'' Raman transitions $|2\rangle \to |1\rangle$ is the same as the rate of the ''forward'' transitions $|1\rangle \to |2\rangle$ and it is given by Eq. (2.3). But the transition rate associated with spontaneous scattering is different since it is described by the Rabi frequency of the classical field

$$R_{sp} \sim \frac{\Omega_R^2\, \gamma_{3\to 1}}{4\, \Delta^2}, \tag{2.9}$$

where $\gamma_{3\to 1}$ is the rate of natural decay in the $|3\rangle \to |1\rangle$ optical transition. In addition to Eq. (2.9), there is also the contribution of spontaneous scattering of the quantum mode via the channel $|2\rangle \to |4\rangle \to |1\rangle$ with a rate equal to R'_{sp} because of the symmetry of the problem.

The important parameter contributed in the expression (2.3) is the light-induced broadening of the ground state Γ determined by all the spontaneous processes including the Rayleigh scattering of both modes. For the most realistic situation when the classical mode has the strongest amplitude the light broadening of the sublevel $|2\rangle$, associated with both the spontaneous processes of Rayleigh and Raman scattering, can be expressed as

$$\Gamma \sim \frac{\Omega_R^2\, \gamma}{4\, \Delta^2}, \tag{2.10}$$

where $\gamma = \gamma_{3\to 1} + \gamma_{3\to 2}$ is the full rate of natural decay of the upper state. While introducing the light-induced broadening, at the same time, we ignore here the other important effect of the light-induced shift of the ground state sublevels. It would be possible to generalize our analysis and to introduce additional light-induced shifts of the Zeeman sublevels. But from the point of view of the method it is easier to discuss the situation when the Zeeman sublevels of two atoms have shifts of the same value but opposite sign. To avoid discussion of the light shift and to recover the original splitting of atomic sublevels we can add to the Hamiltonian of each atom a weak Pauli-type contribution with the magnetic field compensating the effect of the light shift.

For large detuning δ, which has a natural scale either in units of Γ or in units of the quantum field spectral bandwidth $\Delta\omega$, one might expect that the rate of stimulated transitions R would be much less than the rate of spontaneous transitions R'_{sp}. However, in our analysis we assume the detuning δ to be not so large, so it is possible that for a rather strong

classical field the stimulated rate can be made even greater than the spontaneous one. Comparing the corresponding estimations given by expressions (2.3) and (2.7), we can find the acceptable values of the classical Rabi frequency for this. We put off such an estimation here since we will define the range of acceptable variations of all the parameters after we discuss the cooperative Raman scattering by two atoms.

In concluding this section let us make the following remark. In the above analysis of the different terms of perturbation theory we followed a straightforward calculation of Feynman-Keldysh diagrams while assuming an abrupt spectral profile for the quantum radiation. But, if the spectrum of quantum light has a Lorentzian shape and if its spectral bandwidth $\Delta\omega$ is broader than the rate of natural decay γ, then the overlap integral with the atomic Lorentzian can lead to another frequency scale than in the above estimations. For clarity, we will assume that $\Delta\omega < \gamma$ in the case of the Lorentzian spectrum of the quantum radiation. This restriction is really important for us since in our numerical simulations we are going to consider just the Lorentzian spectrum as an example. But it would not be necessary if the spectrum of the radiation had a shape more abrupt than Lorentzian. However, even in the case of a narrow but Lorentzian-type spectrum of quantum light one has to substitute Γ in Eq. (2.3) by $\Delta\omega$ if $\Delta\omega > \Gamma$. This inequality has to be assumed anyway, since it is one of the basic restrictions of the rate constant concept (see [17]). This means that $\Delta\omega$ (not Γ) has to be considered as the natural scale for frequency detuning δ for a Lorentzian spectrum of the quantum light.

B. Cooperative scattering

Since the modes of parametric radiation incident on the atoms are strongly mutually correlated the corresponding scattering events will also be correlated. This means that there is a nonfactorized contribution in the transition amplitude of two atoms considered as joint system. Examples of cooperative scattering are shown in the diagrams in Fig. 2. In these diagrams the energy levels indicate either ground or excited states of the joint system of two atoms. The transition amplitude associated with cooperative scattering can be extracted from the perturbation theory expansion for the two-particle density matrix

$$\rho_{ii',kk'}(\mathbf{r}_1,\mathbf{r}_2;t) = \langle \Psi^{\dagger}_{i'}(\mathbf{r}_1,t)\,\Psi_i(\mathbf{r}_1,t) \times \Psi^{\dagger}_{k'}(\mathbf{r}_2,t)\,\Psi_k(\mathbf{r}_2,t)\rangle. \quad (2.11)$$

Here $\Psi_i(\mathbf{r},t)$ and $\Psi^{\dagger}_i(\mathbf{r},t)$ are the anihilation and creation Heisenberg operators of the atom at the space point $\mathbf{r}$ and in the internal state i (with $i=1,2$). The angular brackets denote averaging over the full initial atom-field density matrix. Since the two atoms are separated by a long distance, the Heisenberg operators relating to different atoms in Eq. (2.11) commute and they can be written in arbitrary order under the averaging.

Strictly speaking, in the Keldysh diagram technique only the time- or antitime-ordered products of the operators are acceptable. Then to introduce the density matrix (2.11) we can evaluate the two-particle Green function

$$W^{(-+)}_{i'i,k'k}(\mathbf{r}'_1t'_1,\mathbf{r}_1t_1;\mathbf{r}'_2t'_2,\mathbf{r}_2t_2) = \langle T_{--++}\,\Psi^{\dagger}_{i'}(\mathbf{r}'_1,t'_1)\,\Psi_i(\mathbf{r}_1,t_1) \times \Psi^{\dagger}_{k'}(\mathbf{r}'_2,t'_2)\,\Psi_k(\mathbf{r}_2,t_2)\rangle \quad (2.12)$$

and then approach the limits $\mathbf{r}'_1\to\mathbf{r}_1$, $t'_1\to t+0$, $t_1\to t$ and $\mathbf{r}'_2\to\mathbf{r}_2$, $t'_2\to t-0$, $t_2\to t$. The ordering operator T_{--++} shows the order of appearance of the Ψ operators in the product according to the well known rules of the Keldysh technique (see Refs. [18–20]). The operators marked by the $+$ sign have to be written first in antiordered sequence and then the operators marked by the $-$ sign have to be written in ordered sequence. The density matrix (2.11) can be expressed by the Green function (2.12) as

$$\rho_{ii',kk'}(\mathbf{r}_1,\mathbf{r}_2;t) = W^{(-+)}_{i'i,k'k}(\mathbf{r}_1t+0,\mathbf{r}_1t;\mathbf{r}_2t-0,\mathbf{r}_2t). \quad (2.13)$$

In the perturbation theory expansion of the Green function (2.12) we have to subtract all the noncoupled contributions describing the Raman scattering by each of the atoms independently, which were discussed in the previous subsection.

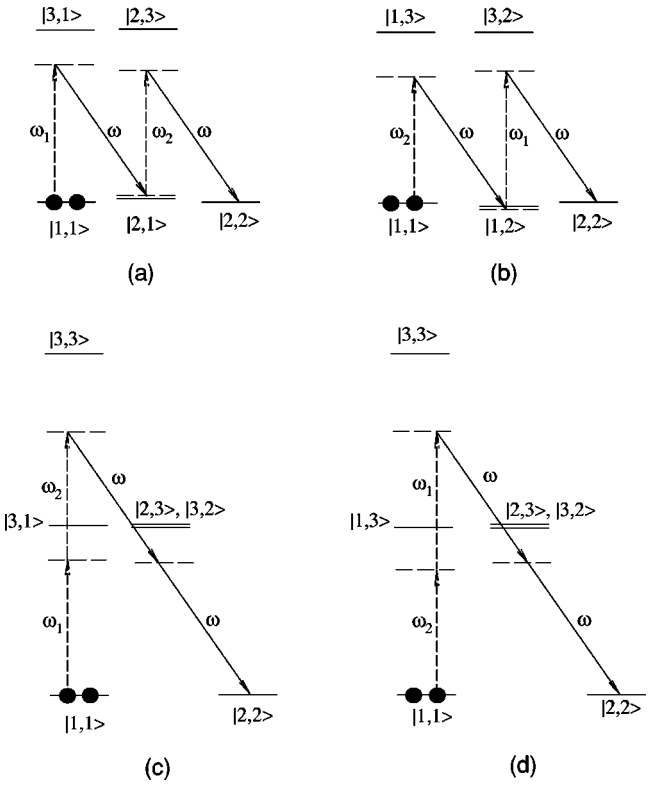

FIG. 2. Examples of cooperative Raman scattering. In these diagrams the energy levels specify the quantum states of the two atoms.

Then in the lowest nonvanishing order of perturbation theory we obtain the following set of coupled diagrams contributed in the Green function $W_{12,12}^{(-+)}(\cdots)$:

$W_{12,12}^{(-+)}(\mathbf{r}_1' t_1', \mathbf{r}_1 t_1; \mathbf{r}_2' t_2', \mathbf{r}_2 t_2) =$

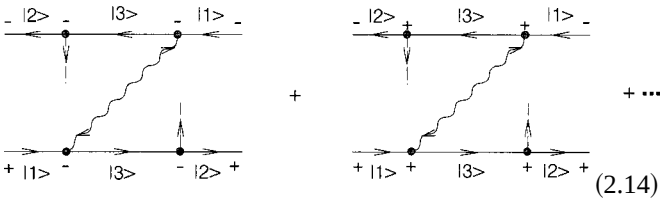

(2.14)

where ellipses denote the other terms expressed by similar diagrams, and internal vertices run over all possible signs. A similar expansion written for the Green function $W_{21,21}^{(-+)}(\cdots)$ would lead to the complex conjugated components of the density matrix (2.11).

As we see from the diagrams (2.14) the two-particle Green function appears here as a coupling of the single-atom Green functions via special waveline describing the anomalous Green function of quantum light. Such a Green function is responsible for the quantum correlation between the twin modes ω_1 and ω_2 of parametric radiation and it is expressed by averaging the pair of annihilation operators

$$\sim\!\!\sim\!\!\sim = \langle \epsilon_1(\mathbf{r}_1, t_1)\, \epsilon_2(\mathbf{r}_2, t_2)\rangle \qquad (2.15)$$

Since these operators commute such a Green function does not depend on the ordering type. Originally this correlation function has a microscopic correlation scale in its dependence on space coordinates as well as on time arguments. However, the OPO modes can propagate through long distances in space. Utilizing a fiber connection one can pass light beams even different laboratories, saving their temporal quantum correlations. Picking out the rapidly oscillating phase factors of the quantum modes, we can introduce the slowly varying component of the anomalous correlation function,

$$\langle \epsilon_1(\mathbf{r}_1, t_1)\, \epsilon_2(\mathbf{r}_2, t_2)\rangle = \exp(ik_1 s_1 - i\omega_1 t_1 + ik_2 s_2 - i\omega_2 t_2)\;\; \phi(t_1 - t_2). \qquad (2.16)$$

Here $s_1 = s_1(\mathbf{r}_1)$ and $s_2 = s_2(\mathbf{r}_2)$ are the optical lengths for the first and second modes, respectively. Strictly speaking the wave vector of the quantum light incident on the atom should be distributed in the the coherence angle of the parametric radiation. However, we can ignore this effect as long as the coherence area of the radiation is greater than the square of its wavelength, and each atom is located inside an area with spatial scale less than a wavelength. The time dependent factor $\phi(t_1 - t_2)$ is actually described by the properties of the source of parametric radiation,

$$\phi(t_1 - t_2) = \langle \tilde{\epsilon}_1(t_1)\, \tilde{\epsilon}_2(t_2)\rangle, \qquad (2.17)$$

where $\tilde{\epsilon}_1(t_1)$ and $\tilde{\epsilon}_2(t_2)$ are the slowly varying Heisenberg operators of the quantum modes.

The correlation function (2.17) possesses the following important property coming from the physical nature of the parametric process. Each elementary event of creation of photon pairs in the general parametric process has to be ordered in time. This means that in the most general situation the correlation function (2.17) can be divided into the sum of two terms,

$$\phi(\tau) = \phi_{\mathrm{I}}(\tau) + \phi_{\mathrm{II}}(\tau), \qquad (2.18)$$

where we approximate

$$\phi_{\mathrm{I}}(\tau) = \langle \epsilon_1 \epsilon_2\rangle_{\mathrm{I}} e^{\tau/\tau_c}\, \theta(-\tau),$$

$$\phi_{\mathrm{II}}(\tau) = \langle \epsilon_1 \epsilon_2\rangle_{\mathrm{II}} e^{-\tau/\tau_c}\, \theta(\tau). \qquad (2.19)$$

Here $\theta(\tau)$ is a step function, which is equal to $+1$ or 0 for $\tau > 0$ or $\tau < 0$, respectively. The correlation time τ_c is responsible for the spectral distribution of quantum radiation: $\Delta\omega \sim \tau_c^{-1}$. The exponential dependence of $\phi_{\mathrm{I}}(\tau)$ and $\phi_{\mathrm{II}}(\tau)$ on time is chosen here as a simple modeling of the real behavior. This exponential approximation is not principally important for our analysis and it is necessary to simplify the numerical procedure. But it is crucial for the following discussion that the complex factors denoted here as $\langle \epsilon_1 \epsilon_2\rangle_{\mathrm{I}}$ and $\langle \epsilon_1 \epsilon_2\rangle_{\mathrm{II}}$ are distinguished by their amplitude and phase. This can lead to possible time ordering in the appearance of the photons: if, for example, $\langle \epsilon_1 \epsilon_2\rangle_{\mathrm{I}} \neq 0$ but $\langle \epsilon_1 \epsilon_2\rangle_{\mathrm{II}} = 0$, the ''blue'' photon will be created in advance of the ''red'' one. It is also possible that $\langle \epsilon_1 \epsilon_2\rangle_{\mathrm{I}} = -\langle \epsilon_1 \epsilon_2\rangle_{\mathrm{II}}$ and we will call such a parametric radiation entangled in time. One example of a light source satisfying the conditions (2.18) and (2.19) is described in the Appendix.

The simple but realistic model of such a light source, described in the Appendix, is valid only if the frequencies of the radiated modes are strongly resolved. That means that the difference between their carrier frequencies $\omega_1 - \omega_2$ should be much greater than their spectral bandwidth $\Delta\omega \sim \tau_c^{-1}$. The light preserves its unique property of time ordering (or entanglement) only for those photon pairs whose detuning from the carrier frequencies is much greater than τ_c^{-1} but at the same time much less than ω_{12}. To make atom 1 interact with the first mode of the entangled pair and atom 2 with the second, we need to split and shift the atomic levels, as shown in Fig. 1(b). The states $|1\rangle$ of the first and second atoms have to be shifted (by means of an external magnetic field) from the states $|2\rangle$ respectively down and up by the same amount comparable with but less than ω_{12}. However, the entire system of two atoms, considered in the shell subspace of the states $|1,1\rangle$ and $|2,2\rangle$, stays degenerate even with the shifted levels of each atom. Moreover, after the stage of optical interaction we can adiabatically switch off the magnetic field and return the system to the fully degenerate state.

If according to our assumption both the atoms initially populate the state $|1\rangle$ then, as follows from the perturbation theory expansion (2.14), after a while there will appear the component of the two-particle density matrix $\rho_{21,21}(t)$, where the pairs of quantum numbers in the subscript relate to the first and second atoms, respectively. This process can be described by the following term in a general master equation for the two-particle density matrix:

$$\frac{\partial}{\partial t}\rho_{21,21}(t)=R_{21,21}\ \ \rho_{11,11}(t), \tag{2.20}$$

where at the beginning $\rho_{11,11}(t)\approx 1$. To simplify the notation we omit here and below the trivial dependence of the density matrix on its space arguments.

To estimate the transition amplitude of the cooperative scattering $R_{21,21}$ one has to consider all the diagrams contributing to Eq. (2.14). However, the leading terms, with minimal energy denominator, just come from the two opening graphs that are shown there. Each of these diagrams describes the appearance of correlation of the atomic coherences $\rho_{21,21}(t)$ depending on whether atoms initially populate sublevel $|1\rangle$ (first graph) or $|2\rangle$ (second graph). The presence of the second graph is caused by the dynamical symmetry of cooperative process. The important peculiarity of these two diagrams is that the internal vertices have one sign in each graph. This means that the diagrams are graphic images of definite types of either time-ordered or antitime-ordered contributions to the series of perturbation theory. They can be interpreted as the opening terms of amplitude or *T*-matrix expansions for the process of atomic (not light) scattering or interaction, where atoms are coupled via entangled modes of quantum light. Then the main contribution to the transition amplitude $R_{21,21}$ coming from the first graph is given by

$$R_{21,21}\approx -i\frac{\Omega_R^2}{16\Delta^2\delta}e^{-2i\vartheta}(\Omega_{\mathrm{I}}'^2-\Omega_{\mathrm{II}}'^2), \tag{2.21}$$

where ϑ is the phase of the classical wave ($\mathcal{E}_0=|\mathcal{E}_0|\exp i\vartheta$), which for the sake of simplicity we assume is the same for both the atoms. The complex magnitudes $\Omega_{\mathrm{I}}'^2$ and $\Omega_{\mathrm{II}}'^2$ are defined as

$$\frac{\Omega_{\mathrm{I}}'^2}{4}=\frac{1}{\hbar^2}d_{31}^2\langle\epsilon_1\epsilon_2\rangle_{\mathrm{I}},$$

$$\frac{\Omega_{\mathrm{II}}'^2}{4}=\frac{1}{\hbar^2}d_{31}^2\langle\epsilon_1\epsilon_2\rangle_{\mathrm{II}}, \tag{2.22}$$

and can be interpreted as the complex correlation Rabi frequencies of the quantum light. Their phases are expressed by the phases of anomalous correlation functions at the OPO output and for the sake of simplicity we assume that $k_1s_1(\mathbf{r}_1)+k_2s_2(\mathbf{r}_2)=2\pi\times$ (any integer). Both the terms in Eq. (2.21) can be visually identified by the diagrams (a) and (b) in Fig. 2.

The expression (2.21) is the important result of this section. In contrast to the transition rates associated with the processes of independent stimulated or spontaneous Raman scattering, the leading term in the cooperative amplitude $R_{21,21}$ *does not depend on any natural decay or broadening rate constants*. This means that in certain conditions if the amplitude $R_{21,21}$ is greater than R, R_{sp}, R_{sp}', or if spontaneous processes are partially eliminated at the beginning stage, when sublevel $|2\rangle$ is not populated, the evolution of the joint system *can be dynamical*, and $R_{21,21}$ will play the role of the coupling constant in the corresponding effective Hamiltonian. If, as in a typical situation, we presume that the classical field has a stronger intensity than the quantum one and $R_{sp}\gg R_{sp}'$, then to approach the inequalities $|R_{21,21}|\gg R$, $|R_{21,21}|\gg R_{sp}'$, $|R_{21,21}|>R_{sp}$ we should subsequently satisfy the conditions

$$\delta\gg\Gamma,\tau_c^{-1},$$

$$\Omega_R\gg\sqrt{\gamma\,\delta},$$

$$|\Omega'|>\sqrt{\gamma\,\delta}, \tag{2.23}$$

where we introduced the full rate of natural decay γ for any upper sublevel $|3\rangle$ or $|4\rangle$. Also in this estimation we substituted $|\Omega_{\mathrm{I}}'|$ and $|\Omega_{\mathrm{II}}'|$ by $|\Omega'|$.

The first and second inequalities in Eq. (2.23) are easy to satisfy but the third one gives us an important physical restriction. It should be noted that the transition dipole moment does not contribute to this inequality, since it comes in both the left and right sides. Canceling it out, the inequality can be rewritten in the form

$$J'\,\lambda\!\!\!^{-2}\,\delta^{-1}>1, \tag{2.24}$$

where J' is the density of the photon flux in the quantum mode and $\lambda\!\!\!^{-}$ is its average wavelength divided by 2π. The inequality (2.24) can be read as follows: the number of photons incident on the atom ($\lambda\!\!\!^{-2}$ is its typical area size in optics) per time interval δ^{-1} should be greater than unity. Since in our assumptions the spectral bandwidth τ_c^{-1} has to be much shorter than the detuning δ, such an inequality can be satisfied only for a strong source of parametric radiation with a high value of the degeneracy parameter. The degeneracy parameter has to be large even though the OPO is assumed to operate in its subthreshold regime. The inequalities (2.23) and (2.24) perform a clear physical restriction: if we need a strong stimulated cooperative process the number of photons initiating the transitions on the time scale δ^{-1} has to be large in the classical as well as in the quantum modes.

In reality only the weak subthreshold OPO generating the photon pairs entangled in time can possess the correlation properties (2.19). A possible example of such a source is described in the Appendix. Even in the ''optimal'' conditions, when $\delta\sim\Gamma\sim\tau_c^{-1}$, it would be impossible to overcome inequality (2.24). It should be noted that in any possible physical situation, when the amplitude of cooperative transitions is greater than either stimulated R or spontaneous R_{sp}' rates of independent Raman transitions $|1\rangle\rightarrow|2\rangle$, the quan-

tum light will be weak and characterized by a small degeneracy parameter. Therefore the inequality (2.24) can never be reached and we can expect only $R_{21,21}<R_{sp}$ and treat the spontaneous rate associated with the coherent mode as an upper estimation for the cooperative amplitude. In practice this means that the evolution of the joint system with initial orientation on one of the Zeeman sublevels can be dynamical only in its beginning stage.

III. TIME EVOLUTION OF THE TWO-PARTICLE DENSITY MATRIX

In this section we discuss the evolution of the two-particle density matrix of the atoms to see how the dynamical stage, described by the Hamiltonian formalism, transforms to the kinetic stage. We compare our qualitative analysis based on the generalized kinetic equation with an exact quantum simulation of the process.

A. Effective Hamiltonian

Consider first the dynamics of the joint system assuming formally that conditions (2.23) and (2.24) can be satisfied, i.e., when the spontaneous processes can be eliminated and the evolution of the two atoms should be governed by cooperative Raman scattering only. If both the atoms initially populate sublevel $|1\rangle$, according to Eq. (2.20) they have the chance to populate sublevel $|2\rangle$ only due to cooperative (not independent) spin flips. The probability of such a flip is proportional to the squared amplitude $R_{21,21}$ and therefore it comes in a higher order of perturbation theory than the coherence $\rho_{21,21}$. Considering all the orders of perturbation theory one can see that at each step of the diagram expansion the joint system will stay in a pure state with the wave function being a superposition of $|1,1\rangle$ and $|2,2\rangle$ cooperative states.

This result can be clearly understood if instead of the transition amplitude we introduce the effective Hamiltonian for the ground state of the atoms in the form

$$\mathcal{H}_{eff}=i\hbar\chi\, s_{+}^{(1)}s_{+}^{(2)}-i\hbar\chi^{*}\, s_{-}^{(1)}s_{-}^{(2)}, \tag{3.1}$$

where $s_{\pm}^{(a)}=\frac{1}{2}(\sigma_x^{(a)}\pm i\sigma_y^{(a)})$ and $\sigma_x^{(a)},\sigma_y^{(a)}$ are the usual Pauli matrices defined for each of the atoms $a=1,2$. The coupling constant χ, which is complex in general, can be recovered by generating the perturbation theory expansion based on the effective Hamiltonian and by comparing it with Eqs. (2.20) and (2.21).

Consider the example of an OPO source entangled in time and described by the correlation Rabi frequencies

$$\Omega_{\mathrm{I}}'^{2}=i|\tilde{\Omega}'|^{2}e^{2i\vartheta},$$

$$\Omega_{\mathrm{II}}'^{2}=-i|\tilde{\Omega}|'^{2}e^{2i\vartheta}, \tag{3.2}$$

which have the same absolute value but opposite signs. We use the tilde here to distinguish the amplitudes of the Rabi frequencies in Eqs. (3.2) and in Eq. (2.5). Then the coupling constant χ is given by

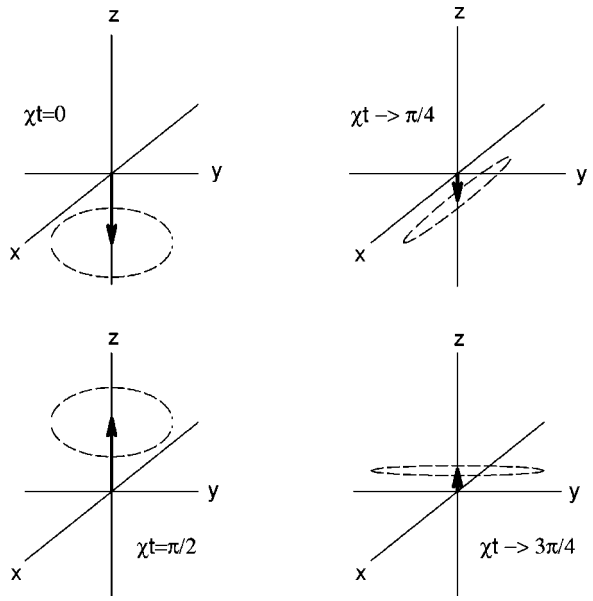

FIG. 3. The time evolution of the cooperative spin for two atoms coupled by effective Hamiltonian (3.1). The elliptic zones in the xy plane show the change of quantum uncertainty for transverse spin fluctuations during the evolution.

$$\chi=\frac{\Omega_R^2}{8\Delta^2\delta}|\tilde{\Omega}|'^{2}. \tag{3.3}$$

This expression has to be considered as the definition of the coupling constant since it is based on and valid only for the the leading term in the expression of the transition amplitude (2.21).

Consider the time dependent Schrödinger equation for the cooperative wave function

$$i\hbar\frac{\partial}{\partial t}|\Psi(t)\rangle=\mathcal{H}_{eff}|\Psi(t)\rangle,$$

$$|\Psi(0)\rangle=|1,1\rangle. \tag{3.4}$$

This equation can be easily solved and its solution is given by

$$|\Psi(t)\rangle=\cos\chi t\,|1,1\rangle+\sin\chi t\,|2,2\rangle, \tag{3.5}$$

which shows that the cooperative quantum state becomes fully entangled at those time moments when $\chi t=\pi/4+\pi/2\times$(any integer) and it possesses a strong spin orientation along the z-axis at $\chi t=\pi/2\times$(any integer). Since we assume $\delta>0$ ($\omega_1>\omega_2$) the coupling constant χ is also positive.

In Fig. 3 we show the time evolution of both the average cooperative spin and its fluctuation. These figures show how the spin-oriented states are changed by the spin-squeezed (entangled) states and vice versa. A less trivial effect here is the following. Because of the squeezing at those time moments when the total spin orientation $\overline{S_z}$ disappears

($\overline{S_z} \to 0$), the ratios $\overline{S_z}/\sqrt{\delta\overline{S_x^2}}$ and $\overline{S_z}/\sqrt{\delta\overline{S_y^2}}$ are $\sqrt{2}$ times higher than the ''standard quantum limit'' defined for states with 100% spin orientation.

B. Generalized kinetic equation

If we include spontaneous processes the evolution of the joint system can be correctly described by density matrix formalism, which is based on the kinetic master equation approach. It is most important for such an approach that the kinetic equation should be written for the two-particle density matrix defined for the entire system of two atoms. Examining all the possible transitions only the following nonzero components of the two-particle density matrix are expected: $\rho_{11,11}$, $\rho_{21,21}=\rho^*_{12,12}$, $\rho_{22,22}$, $\rho_{11,22}$, $\rho_{22,11}$. Ignoring the weak process of independently stimulated Raman scattering and taking into account only those spontaneous transitions that are initiated by the coherent mode, the density matrix components will satisfy the following set of generalized kinetic equations:

$$\dot{\rho}_{21,21}(t) = -\Gamma\,\rho_{21,21}(t) + R_{21,21}[\rho_{11,11}(t) - \rho_{22,22}(t)],$$

$$\dot{\rho}_{22,22}(t) = -2R_{sp}\,\rho_{22,22}(t) + R^*_{21,21}\,\rho_{21,21}(t) + R_{21,21}\,\rho_{12,12}(t),$$

$$\dot{\rho}_{11,11}(t) = R_{sp}\,\rho_{22,11}(t) + R_{sp}\,\rho_{11,22}(t) - R^*_{21,21}\,\rho_{21,21}(t) - R_{21,21}\,\rho_{12,12}(t),$$

$$\dot{\rho}_{22,11}(t) = R_{sp}\,\rho_{22,22}(t) - R_{sp}\,\rho_{22,11}(t),$$

$$\dot{\rho}_{11,22}(t) = R_{sp}\,\rho_{22,22}(t) - R_{sp}\,\rho_{11,22}(t), \tag{3.6}$$

where we introduced on the right side the cooperative contribution defined by Eq. (2.20). For the sake of simplicity we ignore here the light shift effect and consider a degenerate structure of Zeeman sublevels (see the comment in Sec. II A).

The kinetic equations (3.6) have the following important restrictions. First, we call them generalized kinetic equations since it would be impossible to average them over the state of one atom and to introduce the kinetic equations for single-particle density matrices $\rho^{(1)}_{ik}$ or $\rho^{(2)}_{ik}$ defined for the first and second atoms. This follows from the fact that the cooperative contribution leads to the creation of only cooperative coherences $\rho_{21,21}(t)$ and the single-particle coherences of each atom stay equal to zero $\rho^{(1)}_{21}=\rho^{(2)}_{21}=0$. Even in steady state conditions the solution is valid only for the two-particle density matrix, which cannot be factorized into the product of single-particle density matrices.

Secondly, as can be seen from the analysis of the higher order terms in the diagram expansion, these equations have a very narrow area of application. If we want to look at the dynamical stage of evolution we have to solve them only for special initial conditions when the system is put initially in any coherent state in the shell subspace of $|1,1\rangle$ and $|2,2\rangle$ cooperative states. For such a two-dimensional subspace this means that at zero time

$$\rho_{11,11}(0)\rho_{22,22}(0) - |\rho_{21,21}(0)|^2 = 0, \tag{3.7}$$

and only a combination of $\rho_{11,11}$, $\rho_{22,22}$, and $\rho_{21,21}$ obeying Eq. (3.7) can be a candidate for the initial condition. The initial population of $|1,1\rangle$ is the best example, when the spontaneous terms in Eqs. (3.6) are eliminated at the beginning. For this particular case we may either solve the Eqs. (3.6) for the beginning stage, when cooperative process can dominate, or extend the solution up to the steady state regime but considering the final result only as approximate. This restriction comes from the fact that after a while the conditional probabilities $\rho_{11,22}$ and $\rho_{22,11}$ will appear, either because of spontaneous processes caused by the coherent mode or because of the omitted contribution of independent spontaneous and stimulated scattering caused by the weak quantum mode. In turn, this will take the system off the initial subspace and open new possible channels for further evolution. Moreover, in the most general situation it is hard or even impossible to transform the diagram expansions originally written for the Green functions, which depend on many time arguments, to a set of kinetic master equations. But if, as in our basic assumption, the system is put initially in the $|1,1\rangle$ cooperative state and the process of optical pumping caused by the coherent mode is fast enough, the deviation from the actual values of the density matrix components is expected to be small. We will check the validity of the kinetic equations (3.6) by comparing them with the full numerical simulations of the process made in the next subsection.

C. Numerical simulation

The main difficulty for numerical simulation of a process where light is treated as a quantum system comes from the infinite dimension of the field operators. In most practical applications the problem is solved in the framework of the Heisenberg-Langevin formalism (see [17]). The Heisenberg-Langevin equations are written for an atomic subsystem where in addition to dynamical and damping parts there are random sources expressed by quantum field operators. These random sources are typically written and discussed in the Markovian approximation. As far as we know, up to now there have been only few attempts at an exact solution of the quantum problem avoiding the Markovian approximation in Refs. [21–23], in application to a study of the dynamics of the two-level atom in an environment of finite-bandwidth squeezed light.

In the present work we show that the exact dynamics of the density matrix of two four-level atoms interacting with quantum light, as described above, can be recovered from the corresponding analytical solution. By this we mean that in our particular situation any term in any order of the perturbation theory expansion can be calculated analytically, since the chosen correlation functions of quantum light have a quite simple exponential form. It is crucial here that after applying the Wick theorem in any order of perturbation

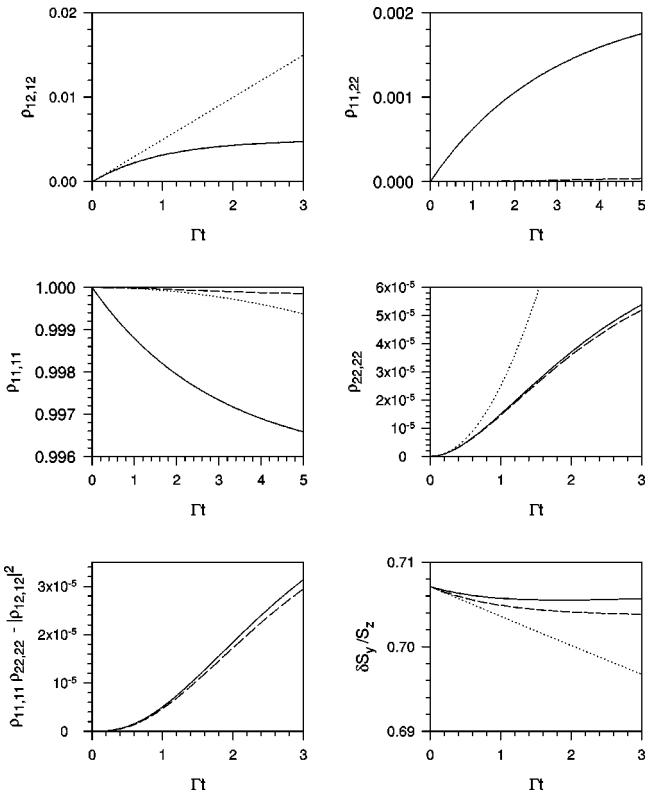

FIG. 4. The temporal behavior of the two-particle density matrix and the squeezing of the cooperative spin calculated for the external parameters $\Omega_R=\gamma$, $\Delta=10^2\gamma$, $\tau_c=10^3\gamma^{-1}$, $|\Omega'|=\sqrt{\gamma/\tau_c}$, $\delta=10^2\tau_c^{-1}$. The exact solution (solid line), the solution of the kinetic equations (3.6) (dashed line), and the the effective Hamiltonian approximation (dotted line) are plotted as functions of time in units of Γ^{-1}.

theory it is possible to evaluate analytically any appearing multiple integral, containing arbitrary products of exponential functions. Of course, in higher orders, while evaluating the large number of multiple integrals created by the Wick theorem, one needs a lot of computer memory to keep the final result. But as follows from our discussion if we are interested to know the evolutionary operator only after rather short time increments, with the goal of estimating the extent of the dynamical stage of evolution, we can restrict our calculations to the lowest orders in interaction with weak quantum modes. At the same time we are able to introduce the exact dressing of the atomic Green functions by interaction with the classical mode as well as with the vacuum continuum. The interaction with the vacuum we consider in Markovian approximation, which is quite reliable in our case. Let us emphasize here that such an *analytical* solution is, in fact, an example of a *numerical* simulation of the process, since the analytical expressions created are too long to write down and can exist only in computer memory.

In Fig. 4 is shown the temporal behavior of all the components of the two-particle density matrix for the following set of external parameters. As a reference frequency scale we use the rate of natural decay of the upper state γ. The Rabi frequency associated with the strong classical field and the frequency detuning from the optical resonance are given, respectively, by $\Omega_R=\gamma$ and $\Delta=10^2\gamma$. The correlation time determining the spectrum of the quantum light is chosen as $\tau_c=10^3/\gamma$. The Rabi frequencies associated with the quantum field and the frequency detuning from the Raman resonance are given by $|\Omega'|=|\tilde{\Omega}'|=\sqrt{\gamma/\tau_c}$ (the same for normal and anomalous correlations) and $\delta=10^2/\tau_c$. Such a choice of $|\Omega'|$ should be considered as an upper estimate, which approximately agrees with the assumption of a weak source of parametric radiation. As can be shown by straightforward calculation, if $|\Omega'|=\sqrt{\gamma/\tau_c}$, the degeneracy parameter for the quantum light has the order of unity. As a scale for the time argument for the dependencies shown in Fig. 4 we use the radiative lifetime of the sublevel 2 associated with spontaneous Rayleigh and Raman scattering of the classical mode, which is denoted as Γ^{-1} [see Eq. (2.10)]. In all the graphs the solid, dashed, and dotted lines correspond, respectively, to the exact solution, solution of the system (3.6), and the effective Hamiltonian approach. All the dependencies were calculated with additional Pauli-type contributions added to the Hamiltonian of each atom in order to compensate the light shift created by the classical mode.

As follows from these graphs there is a quite good agreement between the exact solution and the solution of the set of kinetic equations (3.6) for the cooperative coherence $\rho_{12,12}$ as well as for the cooperative population $\rho_{22,22}$. There is also good agreement for the determinant $\rho_{11,11}\rho_{22,22}-|\rho_{12,12}|^2$ describing approximately the population of the second ''dark'' state in the cooperative subspace. But it is more important that at the initial stage, while the time increment stays less than Γ^{-1}, the exact solution can be approximated by the dynamical solution with good accuracy. In turn this leads to a quite good agreement in the behavior of the cooperative spin and its fluctuation described by the effective Hamiltonian and by the exact solution in the initial stage. The corresponding squeezing dynamics is shown in the last graph in Fig. 4. However, the behavior of the other density matrix components $\rho_{11,22}\approx\rho_{22,11}$ and $\rho_{11,11}$ for the exact solution disagrees with the dynamical as well as with the kinetic approximations. That is clear since both the approximations ignore the spontaneous and stimulated processes of Raman scattering of the weak quantum modes. Such processes demolish the quantum correlations, which can be introduced in the joint system only due to cooperative scattering.

The role of spontaneous Raman scattering of the weak quantum modes can be reduced by increasing both the detuning Δ and the Rabi frequency Ω_R. To show this in Fig. 5 we plot the dependencies on time for all the components of the two-particle density matrix for $\Delta=10^3\gamma$ and for $\Omega_R=10\gamma$. Other parameters are chosen the same as in Fig. 4. For such a choice the amplitude of the cooperative processes as well as the transition rates associated with the independent stimulated Raman scattering of the quantum light and with spontaneous Raylegh-Raman scattering of the classical light have been magnified by the same factor, but the rate of spontaneous Raman transitions associated with the quantum light becomes negligible. As one can see there is no difference between the exact solution and the solution of the kinetic equations (3.6) for $\rho_{12,12}$, $\rho_{22,22}$, and $\rho_{11,11}\rho_{22,22}-|\rho_{12,12}|^2$,

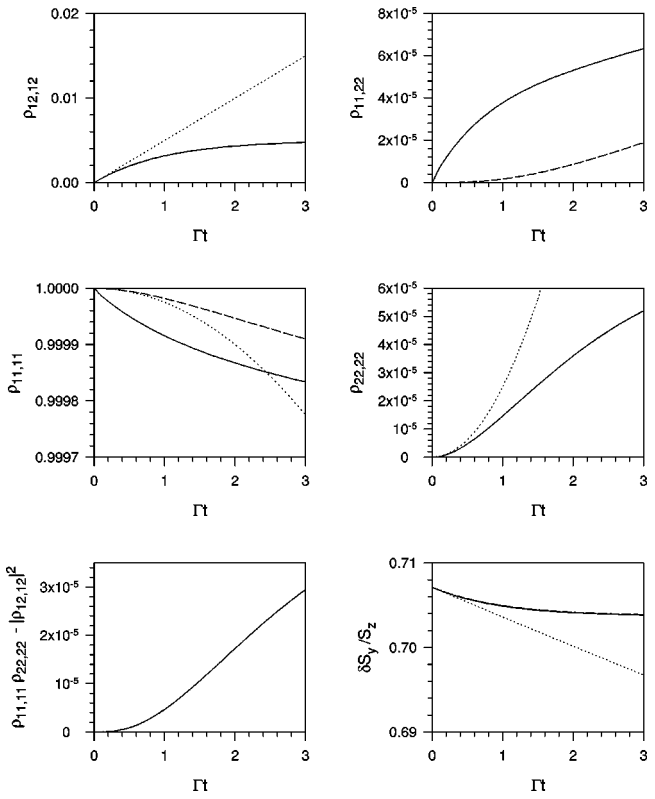

FIG. 5. Same dependencies as in Fig. 4 calculated for $\Omega_R = 10\gamma$, $\Delta = 10^3\gamma$. Other parameters are chosen the same as in Fig. 4.

and also for the squeezing of the cooperative spin $\delta S_y/S_z$. But there is a significant difference in the solutions for the populations $\rho_{11,11}$ and $\rho_{11,22} \approx \rho_{22,11}$. This discrepancy indicates a major limitation of the proposed mechanism of entanglement since the coordinated population of the state $|2,2\rangle$ caused by the cooperative transitions cannot be made greater than the random population of the states $|2,1\rangle$ and $|1,2\rangle$ caused by the independent stimulated Raman transitions. But as follows from our numerical results presented in Figs. 4 and 5 the order of magnitude of the cooperative coherence $\rho_{12,12}$ is much greater than the change in population of all the sublevels.

In concluding this section we point out the following. In the initial stage of its evolution the two-particle density matrix of the joint system can be written in the form

$$\hat{\rho}(t)|_{t \ll \Gamma^{-1}} = p(t)|\Psi\rangle\langle\Psi| + \hat{\rho}', \tag{3.8}$$

where

$$|\Psi\rangle = |\Psi(t)\rangle = c_1(t)|1,1\rangle + c_2(t)|2,2\rangle \tag{3.9}$$

is the normalized entangled wave function of the system. The probability of populating the entangled state approaches unity $p(t) \to 1$ and the important inequality $|c_2| \gg \mathrm{Tr}\,\hat{\rho}'$ must be satisfied. This inequality shows that the populations of all the nonentangled states have a much smaller order of magnitude than the degree of entanglement.

IV. SPATIALLY SEPARATED AND SPIN-ORIENTED MULTIATOMIC ENSEMBLES

The important result of the previous section is as follows. In the initial stage, when the spontaneous processes associated with Rayleigh-Raman scattering of the coherent mode are eliminated, the atoms can make only a cooperative transition between the ground state spin sublevels. The cooperative evolution preserving the coherence in the joint system can be extended only for time increments less than Γ^{-1}. During this period of time both the atoms still stay oriented along the z direction, but there is a small admixture of nondiagonal components of two-particle density matrix, i.e., entanglement. This entanglement manifests itself in the quantum correlation of the transverse spin components of the atoms. But for two atoms this effect is expected to be weak since the spin fluctuations are microscopic. However, if instead of two atoms there were a system of two spatially separated spin-oriented multiatomic ensembles (clouds), then the number of correlations induced by cooperative transitions would be much greater and enhanced by the product $N_1 N_2$, where N_1 and N_2 are the numbers of atoms in the first and in the second cloud, respectively. The magnitude of the induced ''quantum'' contribution to the fluctuations of the macroscopic spin orientation is expected to be of the same order of magnitude as the natural Poissonian scales $\sqrt{N_1}$ and $\sqrt{N_2}$ estimated for the first and second clouds, respectively. Based on the effective Hamiltonian approach, we prove below that in such conditions the system can possess strong quantum correlations of a macroscopic transverse spin components.

Consider a system of two spatially separated atomic ensembles distributed in space in volumes with a typical space length less than λ. The atomic spins in both the ensembles have initial orientation along the z directions. Then during the time $0 < t \ll \Gamma^{-1}$ their evolution can be described by the effective Hamiltonian derived in the previous section. For a multiatomic system the effective Hamiltonian should be rewritten as

$$\begin{aligned}\mathcal{H}_{eff} &= \sum_{a,b} i\hbar\chi\, s_+^{(a)} s_+^{(b)} - i\hbar\chi^*\, s_-^{(a)} s_-^{(b)} \\ &= i\hbar\chi\, S_+^{(\mathrm{I})} S_+^{(\mathrm{II})} - i\hbar\chi^*\, S_-^{(\mathrm{I})} S_-^{(\mathrm{II})},\end{aligned} \tag{4.1}$$

where

$$S_\pm^{(\mathrm{I})} = \sum_{a=1}^{N_1} s_\pm^{(a)}, \quad S_\pm^{(\mathrm{II})} = \sum_{b=1}^{N_2} s_\pm^{(b)}, \tag{4.2}$$

are the collective spin operators of the first (I) and second (II) atomic ensembles. These operators obey the commutation rules

$$[S_+^{(\mathrm{I})}, S_-^{(\mathrm{I})}] = 2S_z^{(\mathrm{I})}, \quad [S_+^{(\mathrm{II})}, S_-^{(\mathrm{II})}] = 2S_z^{(\mathrm{II})}, \tag{4.3}$$

where $S_z^{(\mathrm{I})}$ and $S_z^{(\mathrm{II})}$ are the operators of the collective spins along the z axis, [24].

Let us define the following set of normalized spin operators:

$$a_+^{(\mathrm{I})}=\frac{1}{\sqrt{N_1}}S_+^{(\mathrm{I})},\quad a_-^{(\mathrm{I})}=\frac{1}{\sqrt{N_1}}S_-^{(\mathrm{I})},$$

$$a_+^{(\mathrm{II})}=\frac{1}{\sqrt{N_2}}S_+^{(\mathrm{II})},\quad a_-^{(\mathrm{II})}=\frac{1}{\sqrt{N_2}}S_-^{(\mathrm{II})},\tag{4.4}$$

for which the commutation relations (4.3) transform to the form

$$[a_+^{(\mathrm{I})},a_-^{(\mathrm{I})}]=\frac{2}{N_1}S_z^{(\mathrm{I})}\to -1,$$

$$[a_+^{(\mathrm{II})},a_-^{(\mathrm{II})}]=\frac{2}{N_2}S_z^{(\mathrm{II})}\to -1.\tag{4.5}$$

Here on the right-hand side we show the limits approached for spin-oriented atomic ensembles with $\langle S_z^{(\mathrm{I})}\rangle\approx -N_1/2$, $\langle S_z^{(\mathrm{II})}\rangle\approx -N_2/2$. The commutation relations in the form (4.5) can be treated as follows. In the initial stage of evolution, when the average spin vectors still preserve their initial orientation, the behavior of the ensembles is expected to be similar to a system of two coupled harmonic oscillators. In such an approximation the operators $a_+^{()}$ and $a_-^{()}$ can be considered as the creation and annihilation operators of the oscillators. The coupling is described by the same Hamiltonian as in the model of an ideal nondegenerate optical parametric oscillator,

$$\mathcal{H}_{eff}=i\hbar\tilde{\chi}\,a_+^{(\mathrm{I})}a_+^{(\mathrm{II})}-i\hbar\tilde{\chi}^*\,a_-^{(\mathrm{I})}a_-^{(\mathrm{II})},\tag{4.6}$$

where $\tilde{\chi}=\sqrt{N_1N_2}\chi\gg\chi$ is the constant of nonlinear coupling (parametric interaction) between the oscillators (oscillator modes). It can be seen that by approaching the numbers of atoms in both clouds to macroscopic values the coupling constant $\tilde{\chi}$ can be made greater than the spontaneous rate Γ.

In our assumptions the coupling constant $\tilde{\chi}$ is real and positive [see definition (3.3)]. Then in the interaction representation the canonical operators obey the dependence on time

$$a_-^{(\mathrm{I})}(t)\approx\cosh(\tilde{\chi}t)\,a_-^{(\mathrm{I})}+\sinh(\tilde{\chi}t)\,a_+^{(\mathrm{II})},$$

$$a_+^{(\mathrm{I})}(t)\approx\cosh(\tilde{\chi}t)\,a_+^{(\mathrm{I})}+\sinh(\tilde{\chi}t)\,a_-^{(\mathrm{II})},$$

$$a_-^{(\mathrm{II})}(t)\approx\cosh(\tilde{\chi}t)\,a_-^{(\mathrm{II})}+\sinh(\tilde{\chi}t)\,a_+^{(\mathrm{I})},$$

$$a_+^{(\mathrm{II})}(t)\approx\cosh(\tilde{\chi}t)\,a_+^{(\mathrm{II})}+\sinh(\tilde{\chi}t)\,a_-^{(\mathrm{I})}.\tag{4.7}$$

These dependencies are valid as long as the average collective spins of both the ensembles are approximately equal to their initial values.

As was mentioned above the derived expressions (4.7) can be extended only for the time increment $0<t\ll\Gamma^{-1}$. But even for such a short increment it would be possible to achieve the limit of strong coupling ($\tilde{\chi}t\gg 1$) if the inequality $\tilde{\chi}\gg\Gamma$ were warranted. According to our numerical analysis presented in the previous section, the threshold $\tilde{\chi}\sim\Gamma$ could be overcome for macroscopic numbers of atoms. We can roughly estimate the upper physical limit for the geometric average $\sqrt{N_1N_2}$ by the ratio $\lambda\!\!\!^{-3}/a_0^3$, where a_0 is the Bohr radius, i.e., by the maximal number of atoms that can be inserted in the spatial volume $\lambda\!\!\!^{-3}$. But even if the factor $\sqrt{N_1N_2}$ is much less than this upper estimate the inequality $\tilde{\chi}>\Gamma$ can be overcome and strong quantum correlations between the fluctuations of quadrature components can be observed.

To see this let us define the quadrature components (normalized x and y components of the collective spins) for both the ensembles,

$$X^{(\mathrm{I})}=\frac{1}{2}(a_+^{(\mathrm{I})}+a_-^{(\mathrm{I})}),\quad Y^{(\mathrm{I})}=\frac{1}{2i}(a_+^{(\mathrm{I})}-a_-^{(\mathrm{I})}),$$

$$X^{(\mathrm{II})}=\frac{1}{2}(a_+^{(\mathrm{II})}+a_-^{(\mathrm{II})}),\quad Y^{(\mathrm{II})}=\frac{1}{2i}(a_+^{(\mathrm{II})}-a_-^{(\mathrm{II})}).\tag{4.8}$$

Then we can evaluate their variance

$$\langle X^{(\mathrm{I})2}\rangle=\langle Y^{(\mathrm{I})2}\rangle=\langle X^{(\mathrm{II})2}\rangle=\langle Y^{(\mathrm{II})2}\rangle=\frac{1}{4}\cosh(2\tilde{\chi}t),\tag{4.9}$$

and their mutual correlation functions

$$\langle X^{(\mathrm{I})}X^{(\mathrm{II})}\rangle=\frac{1}{4}\sinh(2\tilde{\chi}t),\quad \langle X^{(\mathrm{I})}Y^{(\mathrm{II})}\rangle=0,$$

$$\langle Y^{(\mathrm{I})}Y^{(\mathrm{II})}\rangle=-\frac{1}{4}\sinh(2\tilde{\chi}t),\quad \langle Y^{(\mathrm{I})}X^{(\mathrm{II})}\rangle=0.\tag{4.10}$$

These correlation properties are typical of the entanglement between continuum variables in a system of two harmonic oscillators. We just need to associate the X variables with coordinates and the Y variables with momenta. As directly follows from these expressions, in the strong coupling limit $\tilde{\chi}t\gg 1$ there will be no variance for the difference $X=X^{(\mathrm{I})}-X^{(\mathrm{II})}$ and for the sum $Y=Y^{(\mathrm{I})}+Y^{(\mathrm{II})}$. So without uncertainty $X\to 0$ and $Y\to 0$.

However, in our case the quadrature components (4.8) have the physical meaning of collective spin fluctuations along the x and y axes, which are normalized to the natural macroscopic scale. Let us come back to the commutation relations (4.3) and point out that the correlation properties (4.10) just describe the quantum correlations created between transverse fluctuations of collective spins. These fluctuations are expected to be much greater (magnified by the factor $[\cosh(2\tilde{\chi}t)]^{1/2}$) than in the case of noninteracting ensembles, but fully correlated along the x axis and anticorrelated along the y axis. For the particular case when the ensembles have equal numbers of atoms ($N_1=N_2$), the difference $S_x^{(\mathrm{I})}-S_x^{(\mathrm{II})}$ and the sum $S_y^{(\mathrm{I})}+S_y^{(\mathrm{II})}$ will approach zero without any quantum uncertainties. In Fig. 6 we show the transformation of the collective spin fluctuations due to the optical interaction.

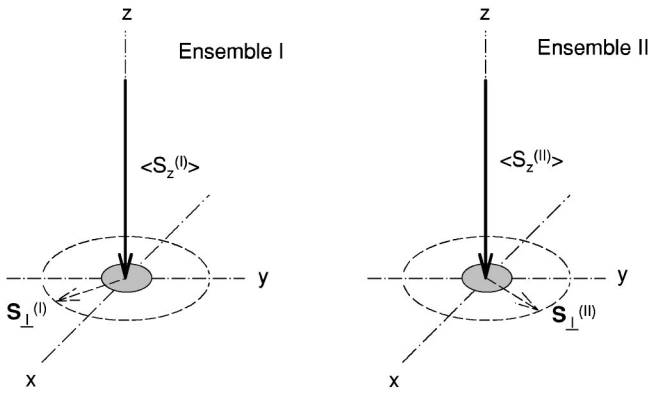

FIG. 6. The original quantum uncertainties of the transverse components of the collective spins, shown as shadowed areas, transform and acquire much greater scale due to the optical interaction. The fluctuations become strongly correlated along the *x* axes and anticorrelated along the *y* axes

Such a pair of identical atomic ensembles entangled over their spin states can be accepted, for example, as an Einstein-Podolsky-Rosen (EPR) system for the quantum teleportation protocol. To show this, consider as input of the teleportation channel any unknown spin state of a third atomic ensemble containing the same number of atoms and characterized by the same average spin orientation along the *z* direction. Then the Bell measurement can be realized as the detection of Faraday rotation of the classical off-resonant and nonsaturating linearly polarized probe light in the balance detection scheme described in Ref. [15]. The probe light beam has to be passed through the third sample and one of the EPR ensembles (say the first), so the rotation angle will be proportional to the random spin orientation (either the sum or difference) of both the atomic samples along the probe beam direction. In this way we can make two measurements of macroscopic spin fluctuations: (1) either the Faraday rotation is associated with a macroscopic spin difference along the *x* direction; or (2) it is associated with the spin sum along the *y* direction. The outer classical signals give us the knowledge of how to add some ''extra'' spin orientation to the second EPR ensemble by the depopulation pumping mechanism (see [10]), via the proper ''extra'' rotations of the polarization plane of the classical linearly polarized light probing the second ensemble along *x* and *y* directions. This light should be identical, from the classical point of view, to the probe light used in the Bell measurements. After all the manipulations, the second EPR ensemble has copied the unknown spin state of the third atomic ensemble.

V. DISCUSSION

In this paper we have described the Raman-type coupling of two four level atoms by parametric radiation which leads to weak entanglement between the Zeeman sublevels in the ground states of these atoms. It seems obvious from the first that the stimulated Raman scattering of fully correlated twin photons of parametric radiation can manifest itself as a cooperative process creating entanglement. However, as follows from our analysis, there are quite strong requirements on the source of the parametric radiation to realize a cooperative spin flip. In this paper we have considered a special light source where the creation of phase conjugated photons of spontaneous parametric scattering would be ordered in time. Then, as has been shown, if the excitation conditions are off resonant for each atom considered independently but resonant for the joint system, the amplitude of stimulated Raman scattering of such light on two distant atoms has to be much greater than the transition rates associated with the usual independent Raman scattering. The light source has quasi-Gaussian statistics and its correlation functions can be modeled by rather simple exponential functions. That allowed us to make a precise numerical simulation of the process based on its full quantum mechanical description. In fact, we have proved numerically that initially spin-oriented atoms would preserve the purity of their quantum state but become entangled after the optical interaction perturbed the system for a short period of time. Unfortunately, because of the negative role of spontaneous processes, it would be impossible to create strong entanglement by extending the duration of the optical coupling.

The important characteristics of parametric radiation are its power, polarization, and spectral properties. In our numerical simulations we considered a quite intensive source of parametric radiation with degeneracy parameter comparable with unity in order of magnitude. Such a bright source of subthreshold parametric radiation is in fact an upper estimate allowing the assumption of an optically thin medium creating this radiation (see the discussion at the end of Sec. II). In reality the quantum radiation is weaker and the cooperative amplitude is smaller, so the dynamical stage of evolution can be extended for a shorter time increment than was shown by our numerical simulations. Since it is hard to preserve the polarization of radiation in fiber it is possible to install additional polarizers in the output before the quantum light is incident on the atoms. This would make less the intensity and magnitude of the Rabi frequencies associated with the quantum light and also reduce the amplitude of the cooperative process. We point out here that all these limitations are typical for any schemes of entanglement based on optical interaction with quantum light.

The important peculiarity of the parametric source considered in this paper is the finite bandwidth of its radiation spectrum. Only for such a light source can we speak about time order in the creation of phase conjugated photons. It was assumed that the output modes of the quantum radiation can be selected by means of any dispersion filter with bandwidth broader than the spectral scale associated with nondegenerate parametric scattering but less than the splitting between corresponding carrier frequencies. However, in application to real experimental conditions it is only necessary to cut off the pumping wave and it is not so important to preselect the ω_1 and ω_2 modes the first and second atoms, as shown in Fig. 1. Since the energy levels of the atoms are shifted in opposite directions, in a cooperative process the atoms themselves can filter these modes. In these conditions all the basic results concerning the entanglement would be retained and it was necessary only to take into account some extra but small contributions associated with the spontaneous

Raman scattering of mode ω_2 by the first atom and of mode ω_1 by the second atom.

Strictly speaking weak quantum correlations (small admixture of entanglement) could be introduced in the system by operating with any weak subthreshold OPO in conditions when the anomalous amplitude correlations of its output modes $\langle \epsilon_1 \epsilon_2 \rangle$ are much greater than the mode populations $\langle \epsilon_1^\dagger \epsilon_1 \rangle$ or $\langle \epsilon_2^\dagger \epsilon_2 \rangle$. An example of an nondegenerate OPO in a cavity, available for experiment and acceptable for theoretical modeling, is described in Ref. [25]. The cooperative amplitude can be made greater than the transition probabilities of independent spin flips as long as the Rabi frequencies associated with anomalous correlations can be made much greater than the normal Rabi frequency associated with the light intensity. However, in the model of Ref. [25] the correlation functions had rather complicated structure, which would make difficult a precise numerical analysis of cooperative Raman transitions in this case.

A small admixture of entanglement in the ground states of two atoms leads to strong entanglement of the transverse macroscopic spin fluctuations of two spatially separated atomic ensembles. To satisfy the phase conditions properly the spatial scale of the atomic ensembles should be made less than the wavelength of the radiation. Let us point out here that this important restriction is caused by the polarization selection of the transition matrix elements (see Fig. 1). If our analysis were presented in a formal model of a Λ-type configuration of atomic levels this restriction would be lost. However, the atoms should be localized in the small spatial volume only during the time of optical interaction. Then the atomic clouds could expand over any macroscopic volume if spin-relaxation processes were eliminated. This circumstance seems important when we look at possible application to the problem of quantum communication between atomic ensembles.

We have to make a special remark concerning the splitting and light shifts of the atomic Zeeman sublevels. The system of degenerate cooperative states $|1,1\rangle$ and $|2,2\rangle$ discussed in this paper is just a convenient approximation for theoretical discussion but it seems a really strong requirement for experimental realization. In a practical experimental situation it is difficult to compensate the different light shifts with high accuracy or to have precise control of the external magnetic field. We hope that, the problem will become less important if we deal with macroscopic ensembles. In such a case we just need to warrant that the remaining discrepancy between the energy splitting in the different ensembles is less than $\tilde{\chi}$. That seems much easier to realize. Also, after the stage of optical coupling is complete the additional external magnetic field can be adiabatically switched off, preserving the entanglement in the system.

ACKNOWLEDGMENTS

We are grateful to E. Polzik for stimulating and fruitful discussions. The financial support of this work was provided in part by the Russian Foundation for Basic Research (RFBR) under Grant No. 01-02-17059. D.V.K. would like to acknowledge financial support from the Delzell Foundation, Inc.

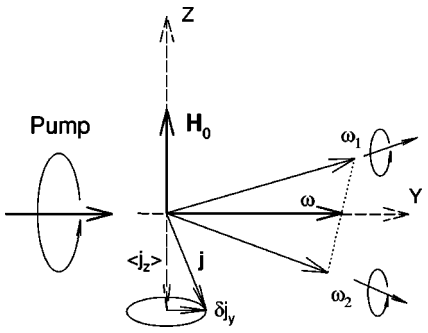

FIG. 7. The geometry of parametric scattering by spin-oriented atomic ensemble. Both the phase conjugated modes of the same circular polarization are created from the pumping wave due to the frequency modulated random gyrotropy of the medium caused by transverse macroscopic spin fluctuations δj_y.

APPENDIX: GENERATION OF TIME-ORDERED PHOTON PAIRS IN FOUR-WAVE PARAMETRIC PROCESS

Here we describe one example of a χ^3 nonlinear medium where creation of the phase conjugated photons in the parametric process is ordered in time. As the basic elementary process we consider spontaneous parametric scattering on an ensemble of atoms polarized in angular momentum and put in an external magnetic field [20]. We will assume the medium to consist of the same atoms as in the body of the paper, i.e., with a 1/2-spin ground state and 1/2-spin excited state. The atoms populate the $m_s = -1/2$ Zeeman sublevel of the ground state and the circularly polarized light probes the atomic ensemble in a direction perpendicular to the magnetic field as shown in Fig. 7. There are several channels interfering in the parametric process, initiated by the pumping (probe) light, which are specified by the diagrams in Fig. 8. The participating transitions are shown here with respect to the coordinate frame with the z axis along the magnetic field. As follows from these diagrams the main peculiarity of the parametric scattering at intermediate energy level is that the ''red'' photon is created in advance of the ''blue'' photon. It is less obvious but can be shown by accurate analysis of the scattering process (see [20]), that in this particular geometry both the phase conjugated photons are created in the same circular polarization as the pumping (probe) wave.

The appearance of the phase conjugated modes can also be interpreted as a random frequency modulation of the probe wave caused by random gyrotropy of the medium, i.e., by transverse macroscopic spin fluctuations δj_y relative to the direction of the average spin orientation $\langle j_z \rangle$. The fluctuations take place at Zeeman frequency. It is important that in such a process the four-wave parametric scattering should be accompanied by spontaneous Raman scattering, as shown in Fig. 9. Then in the first nonvanishing order the anomalous correlation function has the form

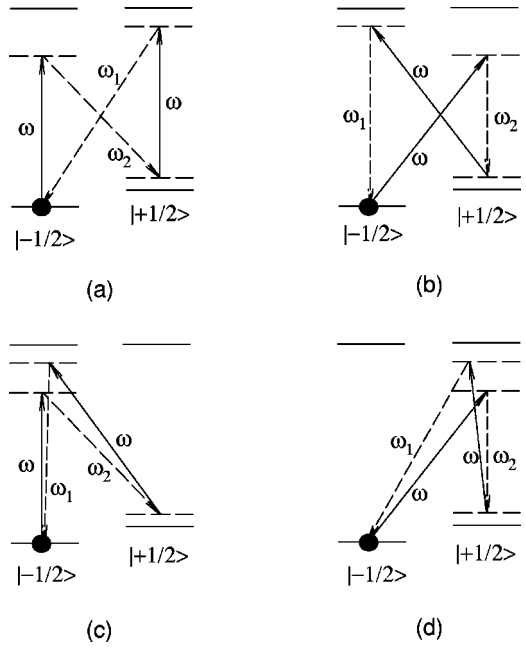

FIG. 8. Diagrams of parametric scattering with respect to a coordinate frame with the z axis along the magnetic field; see Fig. 7.

$$\langle \epsilon(t_1)\epsilon(t_2)\rangle = \langle \epsilon_1\epsilon_2\rangle_{\mathrm{II}}\{\exp[-i\omega_1 t_1 - i\omega_2 t_2 - (t_1-t_2)/\tau_c]\,\theta(t_1-t_2) + \exp[-i\omega_2 t_1 - i\omega_1 t_2 - (t_2-t_1)/\tau_c] \times \theta(t_2-t_1)\}, \tag{A1}$$

where $\omega_1=\omega+\Omega_0$ and $\omega_2=\omega-\Omega_0$ are the carrier frequencies of the parametric radiation and Ω_0 is the frequency of the Zeeman splitting. We choose here the frequency of the pumping wave ω to be the same as the frequency of the coherent mode in the body of the paper in order to approach the resonant condition (2.1). The correlation time τ_c describes the relaxation rate for the spin orientation in the atomic ensemble. In addition to the parametric scattering Raman scattering will occur (see Fig. 9), and the corresponding Stokes component is described by the following normal-type correlation function:

$$\langle \epsilon^{\dagger}(t_1)\epsilon(t_2)\rangle = \langle \epsilon^{\dagger}\epsilon\rangle \exp[i\omega_2(t_1-t_2) - |t_1-t_2|/\tau_c], \tag{A2}$$

which has a spectral location in the vicinity of the carrier frequency ω_2. The external factors $\langle \epsilon_1\epsilon_2\rangle_{\mathrm{II}}$ and $\langle \epsilon^{\dagger}\epsilon\rangle$ have

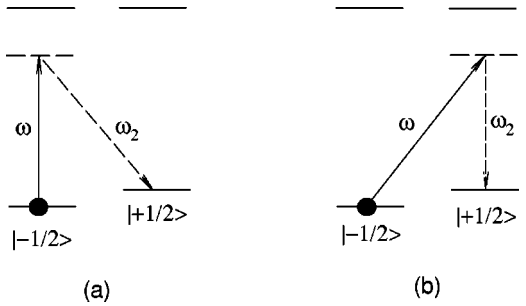

FIG. 9. Diagrams of Raman scattering with respect to a coordinate frame with the z axis along the magnetic field; see Fig. 7.

approximately the same order of magnitude, but the first factor is a complex number those phase depends on the phase of the coherent pumping mode.

Consider a similar atomic ensemble where atoms populate the $m_s=+1/2$ Zeeman sublevel. This leads to inversion in the appearance of the photons of parametric scattering the (''blue'' photon in advance of the ''red'' one) and their anomalous correlation function is given by

$$\langle \epsilon(t_1)\epsilon(t_2)\rangle = \langle \epsilon_1\epsilon_2\rangle_{\mathrm{I}}\{\exp[-i\omega_2 t_1 - i\omega_1 t_2 - (t_1-t_2)/\tau_c]\,\theta(t_1-t_2) + \exp[-i\omega_1 t_1 - i\omega_2 t_2 - (t_2-t_1)/\tau_c] \times \theta(t_2-t_1)\}. \tag{A3}$$

Here the phase of the external factor $\langle \epsilon_1\epsilon_2\rangle_{\mathrm{I}}$ is distinguished from the phase of the similar factor in Eq. (A1). The anti-Stokes component of the Raman scattering is described by the normal-type correlation function

$$\langle \epsilon^{\dagger}(t_1)\epsilon(t_2)\rangle = \langle \epsilon^{\dagger}\epsilon\rangle \exp[i\omega_1(t_1-t_2) - |t_1-t_2|/\tau_c], \tag{A4}$$

which now has a spectral location in the vicinity of the carrier frequency ω_1.

As a possible example of a light source generating a pair of phase conjugated photons entangled in time, we propose the system of two adjacent optically thin atomic media with different spin orientations of their Zeeman sublevels. They have to be excited by the same pumping wave but with different phase conditions for the first and second medium. We assume that the twin modes ω_1 and ω_2, appearing in the parametric process, can be further selected by any dispersion device from the pumping mode ω and then transformed to any proper type of elliptical polarization.

[1] A. Einstein, B. Podolsky, and N. Rosen, Phys. Rev. **47**, 777 (1935); J. Bell, Physics (Long Island City, N.Y.) **1**, 195 (1964).

[2] C.H. Bennett, F. Bessette, G. Brassard, L. Salvail, and J. Smolin, J. Cryptology **5**, 3 (1992).

[3] A.K. Ekert, J.G. Rarity, P.R. Tapster, and G. Massimo Palma, Phys. Rev. Lett. **69**, 1293 (1992).

[4] H. Briegel, W. Dur, S. Van Enk, J.I. Cirac, and P. Zoller, in *Atomic Physics 16*, edited by W.E. Baylis and G.W.F. Drake (AIP, Melville, NY, 1999).

[5] A. Ekert, in *Atomic Physics 14*, edited by D.J. Wineland, C.E. Wieman, and S.J. Smith (AIP, Woodbury, NY, 1994).

[6] C.H. Bennett, G. Brassard, C. Crepeau, R. Jozsa, A. Peres, and W.K. Wootters, Phys. Rev. Lett. **70**, 1895 (1993); D. Bouw-

meester, J. Pan, K. Mattle, M. Eibl, H. Weinfurter, and A. Zeilinger, Nature (London) **390**, 575 (1997).
[7] A. Furusawa, J.L. Sørensen, S.L. Braunstein, C.A. Fuchs, H.J. Kimble, and E.S. Polzik, Science **282**, 706 (1998).
[8] M. Kitagawa and M. Ueda, Phys. Rev. Lett. **67**, 1852 (1991); Phys. Rev. A **47**, 5138 (1993).
[9] A. Kuzmich, K. Mølmer, and E.S. Polzik, Phys. Rev. Lett. **79**, 4782 (1997); J. Hald, J.L. Sørensen, C. Schori, and E.S. Polzik, *ibid.* **83**, 1319 (1999).
[10] W. Happer, Rev. Mod. Phys. **44**, 169 (1972).
[11] A.E. Kozhekin, K. Mølmer, and E.S. Polzik, Phys. Rev. A **62**, 033809 (2000).
[12] L. Vaidman, Phys. Rev. A **49**, 1473 (1994).
[13] S.L. Braunstein and H.J. Kimble, Phys. Rev. Lett. **80**, 869 (1998).
[14] G. Leuchs, T.C. Ralph, C. Silberhorn, and N. Korolkova, J. Mod. Opt. **46**, 1927 (1999).
[15] L.M. Duan, J.I. Cirac, P. Zoller, and E.S. Polzik, e-print quant-ph/0003111.
[16] Throughout the paper we use the term OPO for any source of spontaneous parametric scattering, which can be either a down-conversion process or four-wave mixing in a χ^3 nonlinear medium.
[17] C. Cohen-Tannoudji, J. Dupont-Roc, and G. Grynberg, *Atom-Photon Interactions: Basic Processes and Applications* (John Wiley & Sons, Inc., New York, 1992).
[18] L.V. Keldysh, Zh. Éksp. Teor. Fiz. **47**, 1515 (1964) [Sov. Phys. JETP **20**, 1018 (1965)].
[19] E.M. Lifshitz and L.P. Pitaevskii, *Course of Theoretical Physics: Physical Kinetics* (Pergamon Press, Oxford, 1981).
[20] D.V. Kupriyanov and I.M. Sokolov, Zh. Éksp. Teor. Fiz. **99**, 93 (1991) [Sov. Phys. JETP **72**, 50 (1991)]; V.V. Batygin, D.V. Kupriyanov, and I.M. Sokolov, Quantum Semiclassic. Opt. **9**, 559 (1997).
[21] A.S. Parkins, Adv. Chem. Phys. **85**, 607 (1993).
[22] A.S. Parkins and C.W. Gardiner, Phys. Rev. A **37**, 3867 (1988).
[23] H. Ritsch and P. Zoller, Phys. Rev. A **38**, 4657 (1988).
[24] Strictly speaking, to satisfy the phase conditions properly and to define an effective Hamiltonian in the form (4.1) it is enough to put the atoms of each ensemble in a volume with rather short length (less than λ) only along the directions associated with the wave vectors of the quantum and classical modes. The cloud may have arbitrary length along the direction orthogonal to both these wave vectors; see the excitation geometry displayed in Fig. 1(a) in the case of two atoms.
[25] P. Lock, S.L. Brounstein, and H.J. Kimble, e-print quant-ph/9902030.